

Commensurate Itinerant Antiferromagnetism in BaFe_2As_2 : ^{75}As -NMR Studies on a Self-Flux Grown Single Crystal

Kentaro KITAGAWA*, Naoyuki KATAYAMA, Kenya OHGUSHI, Makoto YOSHIDA, and Masashi TAKIGAWA

Institute for Solid State Physics, University of Tokyo, 5-1-5 Kashiwanoha, Kashiwa, Chiba 277-8581, Japan

We report results of ^{75}As nuclear magnetic resonance (NMR) experiments on a self-flux grown single crystal of BaFe_2As_2 . A first-order antiferromagnetic (AF) transition near 135 K was detected by the splitting of NMR lines, which is accompanied by simultaneous structural transition as evidenced by a sudden large change of the electric field gradient tensor at the As site. The NMR results lead almost uniquely to the stripe spin structure in the AF phase. The data of spin-lattice relaxation rate indicate development of anisotropic spin fluctuations of the stripe-type with decreasing temperature in the paramagnetic phase.

KEYWORDS: BaFe_2As_2 , NMR, itinerant antiferromagnetism, ternary iron arsenide

1. Introduction

The discovery of high temperature superconductivity in the layered oxypnictide compound $\text{LaFeAsO}_{1-x}\text{F}_x$ by Kamihara *et al.*¹ with the superconducting transition temperature $T_c = 26$ K has opened new opportunities to investigate interplay between magnetism and superconductivity. The unsubstituted compound LaFeAsO undergoes successive phase transitions: a tetragonal to orthorhombic structural transition at 155 K² followed by an antiferromagnetic (AF) transition at 142 K.³ These transitions are suppressed by substituting oxygen with fluorine, leading to the superconductivity. Higher T_c exceeding 50 K was achieved by substituting La with other rare earth elements.^{4,5}

Subsequent synthesis of a new ternary series of superconductors without oxygen, $A_{1-x}B_x\text{Fe}_2\text{As}_2$ ($A=\text{Ba}, \text{Sr}, \text{Ca}$; $B=\text{K}, \text{Na}$)⁶⁻⁹ has marked a further important step. For these materials, large single crystals can be grown by flux methods, which is crucial to investigate anisotropic properties of the layered superconductors and to determine the paring symmetry. Here again, the unsubstituted materials show both the structural and the AF transitions but at the same temperature. For example, BaFe_2As_2 has a tetragonal structure with the space group $I4/mmm$ at room temperature. The structural transition to the orthorhombic $Fmmm$ space group and the AF transition into a stripe-type order take place simultaneously near 140 K.^{6,10} Superconductivity emerges by substituting Ba with K, which suppresses the structural and the AF transitions. Whether the structural instability or magnetic fluctuations (or both) plays vital role for the occurrence of superconductivity is an important issue to be addressed by various microscopic experiments.

In this paper, we report nuclear magnetic resonance (NMR) studies on ^{75}As nuclei in a single crystal of BaFe_2As_2 grown in FeAs flux. NMR is a powerful tool, sensitive to both the magnetism and the local structure. We observed a discontinuous splitting of the NMR lines below 135 K, indicating a first-order AF transi-

tion. A simultaneous tetragonal-to-orthorhombic structural transition was detected by a sudden change of the quadrupole splitting in the NMR spectra, indicating substantial change in the local charge distribution around the As sites. Observation of the internal field parallel to the c -axis in the AF state leads nearly uniquely to the stripe-type spin structure with the AF moment perpendicular to the stripe. The temperature dependence of the spin-lattice relaxation rate ($1/T_1$) indicates development of anisotropic spin fluctuations of stripe-type in the paramagnetic tetragonal phase.

2. Experiment

The sample used in our NMR experiment was prepared by the self-flux method. To avoid contamination by external elements, we chose FeAs as the flux after Wang *et al.*¹¹ The starting materials were mixed in a graphite crucible with the ratio $\text{Ba}:\text{Fe}:\text{As}=1:4:4$ and sealed in a double quartz tube with argon gas. The tube was heated up to 1100°C in 14 hours (including the holding at 700°C for 3 hours) and slowly cooled down to 900°C in 50 hours. The resistivity and the magnetic susceptibility showed a sharp transition at ~ 135 K, in agreement with the results by Wang *et al.*¹¹

For the NMR experiments, a crystal with the size $3 \times 2 \times 0.05$ mm³ was mounted on a probe equipped with a two-axis goniometer. This allows fine alignment of arbitrary crystalline axis along the magnetic field within $\sim 0.2^\circ$. The field-swept NMR spectra were taken by Fourier transforming the spin-echo signal with the step-scan technique. The Knight shift and the spin-lattice relaxation rate (T_1^{-1}) were measured at the fixed field of 6.615 T. The value of T_1^{-1} was determined by fitting the time dependence of the spin-echo intensity of the central transition line after the inversion pulse to the theoretical formula.¹² Good fitting was obtained above 20 K. At lower temperatures, an extra component with short T_1 caused slight deviation, which is likely due to residual disorder.

Prior to the synthesis of the self-flux grown crystals, we also grew crystals with Sn-flux.¹³ However, the energy dispersive x-ray fluorescence (EDX) spectroscopy

*kitag@issp.u-tokyo.ac.jp

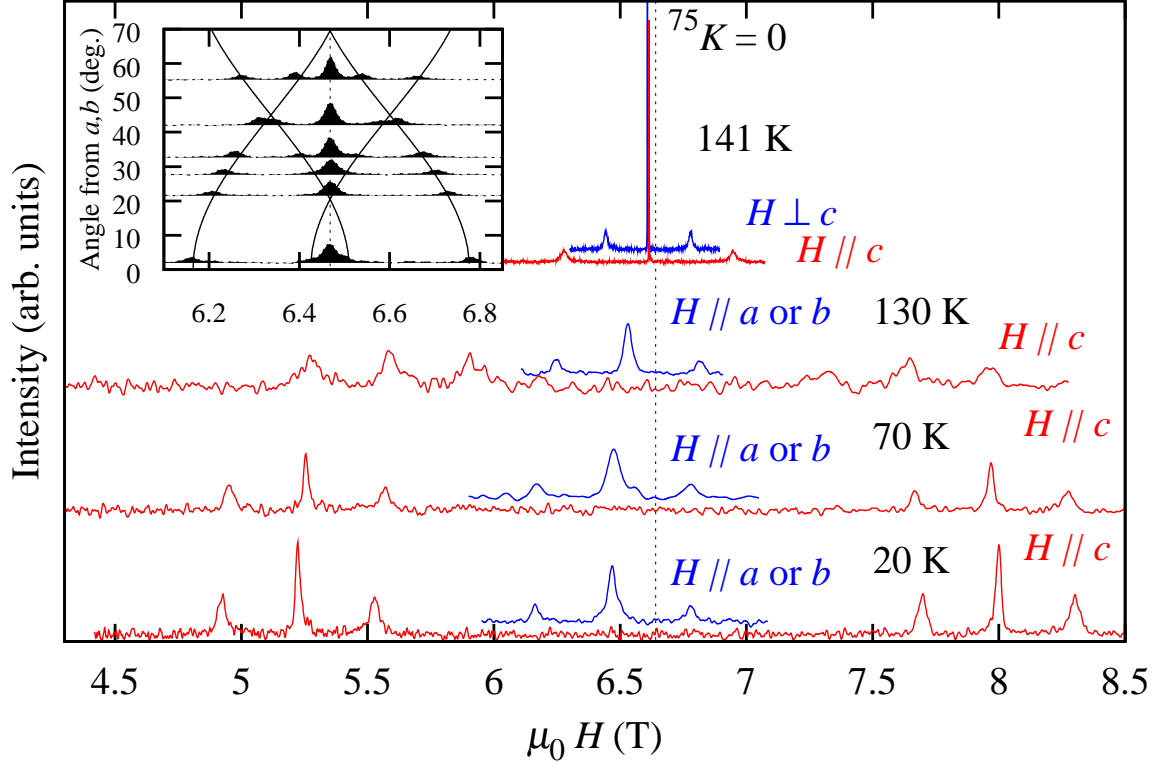


Fig. 1. (Color online) ^{75}As -NMR spectra obtained by sweeping the magnetic field at the fixed frequency of 48.41 MHz. In the paramagnetic state at 141 K, the spectrum consists of a sharp central line and two broader satellite lines. Below 135 K, the internal fields along the c -axis due to commensurate AF order splits the NMR spectra for $H \parallel c$ (red lines) and shifts the spectra to lower fields for $H \parallel a$ - or b -axis (blue lines). The inset shows angular variation of the NMR spectrum at 20 K for the field rotated in the ab -plane. The two sets of satellite lines originate from the twinned structural domains in the orthorhombic phase. The satellite positions are fitted to Eq. (1) with the quadrupole parameters: $\nu^c = 2.21$ MHz, $|\nu^a - \nu^b|/|\nu^c| = 1.18$ (solid lines).

revealed 1.5% content of Sn substitution and the transition temperature detected by resistivity measurement was reduced to ~ 70 K. Also the NMR spectra were extremely broad.

3. Experimental Results

The main panel of Fig. 1 shows ^{75}As -NMR spectra at the fixed frequency of 48.41 MHz obtained by sweeping the magnetic field parallel and perpendicular to the c -axis at several different temperatures. The spectra at $T=141$ K are representative of the paramagnetic phase, while the spectra at the other temperatures belong to the AF ordered phase.

As ^{75}As nuclei have spin 3/2, the NMR frequencies ν are generally expressed by a perturbation series when the magnetic Zeeman interaction dominates over the quadrupole interaction,

$$\begin{aligned} \nu_{m \leftrightarrow m-1} = & \mu_0 {}^{75}\gamma H_{\text{eff}} \\ & + \frac{1}{2}\nu^c \left(m - \frac{1}{2} \right) \left(3 \cos^2 \theta - 1 \right. \\ & \left. + \frac{\nu^a - \nu^b}{\nu^c} \sin^2 \theta \cos 2\phi \right) \\ & + (\text{2nd order correction}). \end{aligned} \quad (1)$$

The first term is the Zeeman frequency, where ${}^{75}\gamma = 7.29019$ MHz/T is the nuclear gyromagnetic ratio and H_{eff} is the effective field at the As nuclei. In the paramagnetic state, the effective field is expressed as $H_{\text{eff}} = (1 + K^i)H$, where H is the external field and K^i is the Knight shift along the i -axis. The second term represents the first order quadrupolar shift for the three nuclear transitions $I_z = m \leftrightarrow m - 1$ ($m = 3/2, 1/2, \text{ or } -1/2$). The explicit expression for the second order correction can be found in a standard textbook.¹⁴ The quadrupole splitting parameters ν^i ($i = a, b, c$) are related to the electric field gradient (EFG) tensor $V_{\alpha\beta} = \partial^2 V / \partial r_\alpha \partial r_\beta$ at the As nuclei as $\nu^i = eV_{ii}Q/2h$, where Q is the nuclear quadrupole moment of ^{75}As . Here the crystal axes are defined with respect to the orthorhombic ($Fm\bar{3}m$) unit cell. Note that the $mm2$ symmetry of the As sites in the orthorhombic phase guarantees that the crystalline a , b , and c axes are the principal axes of EFG tensor. The polar angle (θ, ϕ) specifies the direction of the magnetic field relative to the crystalline axes. In the tetragonal phase, the NMR spectrum is independent of ϕ since $\nu_a = \nu_b = -\nu_c/2$.

As shown in Fig. 1, the NMR spectra at $T=141$ K show a sharp central line ($m=1/2$) with the full width at half maximum (FWHM) of 3.5 kHz and two broader satellite lines ($m = 3/2$ and $-1/2$) with the FWHM of

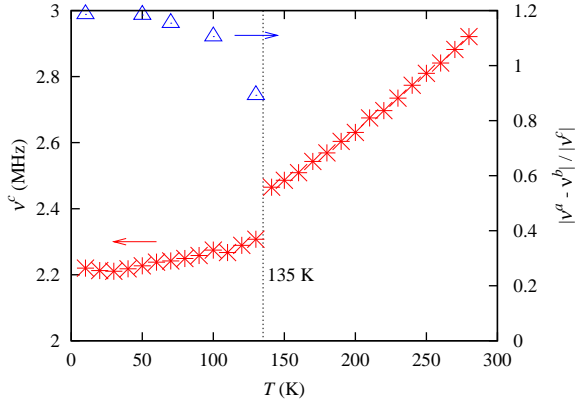


Fig. 2. (Color online) Nuclear quadrupole splitting frequency along the c axis, ν^c , and the asymmetry parameter $|\nu^a - \nu^b|/|\nu^c|$ are plotted as a function of temperature. The asymmetry parameter is zero in the tetragonal phase. Its emergence below 135 K and a jump in ν^c indicate the first-order structural transition into the orthorhombic phase.

100 kHz. We emphasize that the crystal grown in Sn-flux exhibits much broader lines (the FWHM is 150 kHz for the central line and 500 kHz for the satellite lines), indicating substantial disorder caused by the substituted Sn. The quadrupole splitting ν_c is determined from the separation between the two satellite lines for $H \perp c$ ($\theta = \pi/2$), which is a half of the separation for $H \parallel c$ ($\theta = 0$) as expected. The value of ν_c is plotted against temperature in Fig. 2.

The Knight shift ${}^{75}K$ was determined from the resonance position of the central line after correcting for the demagnetization field and the second order quadrupolar shift. The temperature dependence of ${}^{75}K$ is shown in the inset of Fig. 3 for $H \parallel c$ and for $H \perp c$ above 140 K. For both directions, ${}^{75}K$ decreases slightly with decreasing temperature. This temperature dependence agrees with the earlier data on a crystal grown in Sn-flux by Baek *et al.*¹⁵ and on a powder sample by Fukazawa *et al.*¹⁶ However, there are some discrepancies in the absolute values of the Knight shift. In general, the Knight shift consists of the T -dependent spin shift, and the T -independent chemical (orbital) shift.

$$K(T) = K_{\text{chem}} + K_{\text{spin}}(T). \quad (2)$$

Likewise the susceptibility is the sum of the contributions from core diamagnetism, orbital (van Vleck) paramagnetism, and spin paramagnetism,

$$\chi(T) = \chi_{\text{dia}} + \chi_{\text{orb}} + \chi_{\text{spin}}(T). \quad (3)$$

The spin shift is linearly related to the spin susceptibility via the hyperfine coupling constant A_{spin} ,

$$K_{\text{spin}}(T) = A_{\text{spin}}\chi_{\text{spin}}(T)/N_A\mu_B. \quad (4)$$

We have indeed observed linear relations between ${}^{75}K$ and the magnetic susceptibility as displayed in the main panel of Fig. 3. The slope of these plots gives the values of the spin hyperfine coupling constant as ${}^{75}A_{\text{spin}}^a = 2.64 \pm 0.07$ T/ μ_B , and ${}^{75}A_{\text{spin}}^c = 1.88 \pm 0.06$ T/ μ_B .

However, these values must be taken with caution. Since $\chi_{\text{dia}} \sim -6 \times 10^{-5}$ (emu/mol-Fe) and χ_{orb} should

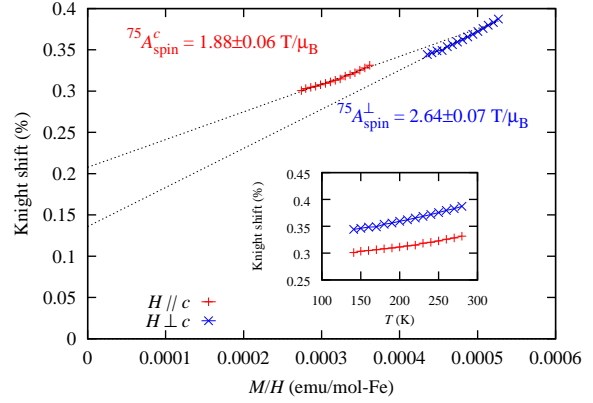


Fig. 3. (Color online) Inset: the temperature dependence of the Knight shift ${}^{75}K$ for the field parallel and perpendicular to the c -axis. Main panel: ${}^{75}K$ is plotted against the bulk susceptibility χ measured by Wang *et al.*¹¹ The dotted lines represent the fits to a linear relation.

be of the order of 1×10^{-4} (emu/mol-Fe), we expect K_{chem} to be larger than the y -intercept of the K - χ plots in Fig. 3. Although not much data are available for the chemical shift of As compounds, the value $K_{\text{chem}} \sim 0.2\%$ appears to be anomalously large. Therefore, we cannot rule out the possibility that the hyperfine coupling is changing as a function of temperature. If this is the case, the true values of $A_{\text{spin}}(T)$ should be even larger than given above.

When the temperature is lowered below 135 K, the NMR spectrum develops a two-fold splitting for $H \parallel c$, doubling the number of resonance lines (Fig. 1). This is the direct evidence for a two-sublattice AF order, consistent with the earlier Mössbauer⁶ and neutron¹⁰ experiments. The AF moments generate a spontaneous internal field with alternating sign $\pm\Delta$, therefore, $H_{\text{eff}} = H \pm \Delta$ in Eq. (1). The commensurate AF order has been reported previously by Fukazawa *et al.* based on the ${}^{75}\text{As}$ -NMR spectrum at zero magnetic field.¹⁶ The temperature dependence of Δ determined from the separation between the split center lines is shown in Fig. 4 by crosses. On the other hand, no splitting was observed when the field is applied along the a - or b -axis. Instead the whole spectrum is shifted to lower fields (Fig. 1). This indicates that the internal field is parallel to the c -axis. When $H \perp c$, H_{eff} is given by the magnitude of the vector sum of the mutually orthogonal external and internal fields, $H_{\text{eff}} = \sqrt{H^2 + \Delta^2}$, giving positively unsplit resonance lines. This allows us to determine Δ also from the shift of the central line for $H \parallel a$ or b , as indicated by squares in Fig. 4. The values of Δ for the two field orientations show good agreement, indicating that the magnitude and the direction of the AF moment are independent of the field direction.

We have studied the behavior in the vicinity of the phase transition by recording the peak intensity of the Fourier transformed spectrum at the resonance position of the paramagnetic phase with changing temperature as shown in the inset of Fig. 4. The magnetic transition was found to be very sharp with the transition width less than 1 K, indicating good homogeneity of our crystal. It also

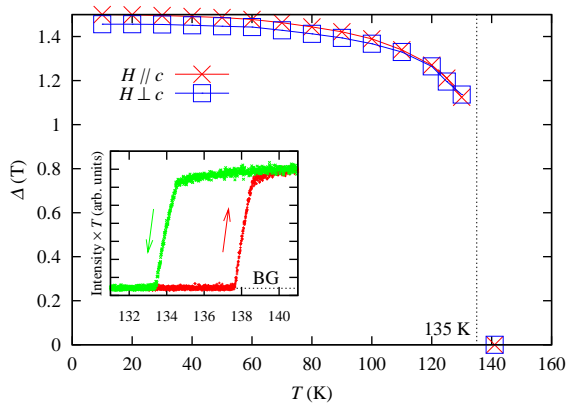


Fig. 4. (Color online) The temperature dependence of the internal field Δ at the As nuclei associated with the antiferromagnetic order. The inset shows the intensity of the central line at the resonance position of the paramagnetic phase for $H \perp c$. The abrupt change with hysteresis is the evidence for the first-order magnetic transition.

shows a clear hysteresis in temperature about 4 K wide, providing conclusive evidence for the first-order transition. This is also inferred from the discontinuous development of the internal field. Let us remark that the crystal grown in Sn-flux shows much broader transition and extremely large line width (2 MHz) in the AF phase even though the magnitude of the internal field below 20 K is the same as observed for the self-flux grown crystal.

We have also confirmed a discontinuous structural transition by a pronounced change of symmetry of EFG. As shown in the inset of Fig. 1, the quadrupole splitting at 20 K varies with the field direction (ϕ) in the ab -plane, indicating that $\nu^a \neq \nu^b$. This is consistent with the orthorhombic symmetry. The angular variation of the NMR spectra displayed in the inset of Fig. 1 shows two branches of satellite lines, which are shifted by 90° . This comes from the twinned orthorhombic domains. The ϕ dependence of the satellite lines can be fit to Eq. (1). The extrema of the angular variation correspond to the field directions parallel to either a - or b -axis. Note, however, that we cannot determine which branch corresponds to the a - or b -axis. The asymmetry parameter of EFG defined by $|\nu^a - \nu^b|/|\nu^c|$ is plotted in Fig. 2. The asymmetry parameter, which is zero in the tetragonal phase, develops abruptly below the transition temperature. A jump in ν_c is also observed across the transition. These results establish the simultaneous structural and magnetic transition.

What is most surprising is the large value of asymmetry parameter exceeding one in the low temperature phase. This means that the principal axis for the largest EFG changes by 90° across the transition. Since the orthorhombicity of the lattice constant (b/a) is less than 1%,⁶ such a drastic change of EFG must be caused by substantial change of the charge density distribution around the As sites. This suggests that the band structure or the nature of the Fe-As bonds becomes highly anisotropic in the ab -plane. We also notice anomalously large temperature variation of ν_c in the paramagnetic phase. Nearly 20% reduction of ν_c from 300 K to 140 K is

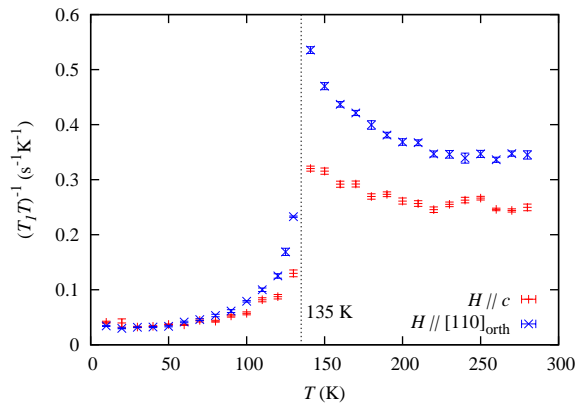


Fig. 5. (Color online) Nuclear spin-lattice relaxation rate divided by temperature, $(T_1T)^{-1}$, is plotted as a function of temperature for two field-orientations. The behavior, $T_1T = \text{const.}$, at low temperatures indicates the itinerant (Fermi liquid) character of the material. We should remark that the upturn of (T_1T) in the paramagnetic phase is observed only for $H \perp c$. This indicates anisotropic development of the stripe-type antiferromagnetic spin fluctuations perpendicular to both the c -axis and the stripe.

clearly beyond (and in the opposite direction from) what is expected from normal thermal lattice contraction, indicating large variation in the local charge distribution

Finally, we show the spin-lattice relaxation rate divided by temperature $(T_1T)^{-1}$ in Fig. 5. In the paramagnetic phase, $(T_1T)^{-1}$ shows anisotropic temperature dependence. Substantial enhancement is seen for $H \parallel a$ or b with decreasing temperature, while $(T_1T)^{-1}$ is nearly constant for $H \parallel c$. Across the first order structural/magnetic transition, $(T_1T)^{-1}$ drops discontinuously by a factor of three. At low temperatures, $(T_1T)^{-1}$ approaches a constant value for both field orientation expected for a Fermi liquid. This is consistent with the metallic behavior of the resistivity. Thus the low temperature phase is characterized as an itinerant antiferromagnetic phase. Although the AF order may be driven by Fermi surface nesting, our results demonstrate that the order is commensurate and a sizable density of states at the Fermi level remains down to $T = 0$.

4. Discussion

Let us first discuss the nature of hyperfine interaction between As nuclei and Fe spins. Generally this is the sum of the dipolar interaction and the transferred hyperfine interaction. While the former is long ranged, the latter involves hybridization between the Fe-3d and As-4s, 4p orbitals and it is usually sufficient to consider only the nearest neighbor interaction. Since As-Fe bonds form nearly perfect tetrahedra, the dipolar field becomes extremely small, at most 0.01 T/ μ_B along the c -direction and a half of this value perpendicular to the c -direction. This is two orders of magnitude smaller than the experimental coupling constants in the paramagnetic state. Therefore, dominant contribution comes from the transferred hyperfine fields.

We now consider the spin structure in the AF ordered state which is compatible with the ^{75}As -NMR spectra.

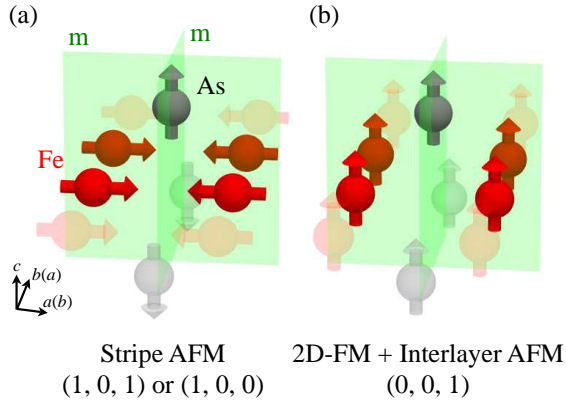


Fig. 6. (Color online) Possible spin configurations in the AF ordered state in BaFe₂As₂, which is compatible with the ⁷⁵As-NMR results. Only one Fe-As layer is drawn for simplicity. The internal field at the As sites are shown by grey arrows. There are two candidates: (a) the stripe AF order and (b) AF stacking of the ferromagnetic layers. The former case (a) is realized in BaFe₂As₂ (see text).

There are two major experimental constraints: (i) the internal field at the As sites is parallel to the *c*-axis and (ii) The AF state has a simple two-sublattice structure. The formal symmetry analysis of the hyperfine field for various AF spin structure is presented in the Appendix, where we demonstrate that there are two possible spin structure compatible with the NMR experiments as shown in Fig. 6. More intuitively, by considering the dipolar field from Fe spins, one can understand that only these two configurations generate a finite *c*-component of the internal field. In the first configuration (a), the AF order is described by the wave vector (101) or (100), forming stripes with the AF moments directed perpendicular to the stripe. (Note that we cannot distinguish the orthorhombic *a*- and *b*-axes by NMR spectra.) In the second configuration (b), ferromagnetic layers in the *ab*-plane stack antiferromagnetically along the *c*-axis. The second structure, however, is highly unlikely since the temperature dependence of the susceptibility rules out ferromagnetic correlation.

The above conclusion is fully consistent with the results of neutron diffraction experiment on BaFe₂As₂,¹⁰ SrFe₂As₂,¹⁷ and CaFe₂As₂.¹⁸ The AF order is described by the wave vector (101) in the orthorhombic structure. The AF moment is found to be parallel to the *a*-axis. Note that the internal field along the *c*-axis at the As nuclei is generated only by the *a*-component of the AF moment (see the arguments in the Appendix). Therefore, only the anisotropic (off-diagonal) part of the hyperfine interaction can be relevant. For example, the isotropic Fermi contact interaction from the As-4*s* orbital, which should be the dominant source of the transferred hyperfine interaction in the paramagnetic phase, does not contribute to the internal field in the AF ordered phase. A possible origin for such anisotropic hyperfine field is the dipolar field from the AF moments, which is calculated to be 0.25 T/ μ_B for the stripe spin structure. Concerning the magnitude of the ordered moment, it is estimated to

be 0.89 μ_B from the neutron experiments,¹⁰ while much smaller value 0.4 μ_B was proposed from the Mössbauer experiments.⁶ Even if we take the larger value of 0.9 μ_B , the dipolar field from the AF moments is nearly an order of magnitude smaller than the experimental value. Therefore, the anisotropic hyperfine field from the AF moment must come from the hybridization between the Fe-3*d* and the As-4*p* orbitals. We should also recall that highly anisotropic charge density distribution associated with the Fe-As bonds is detected by the asymmetric EFG in the orthorhombic phase. We suspect such anisotropic nature of the Fe-As hybridization in the orthorhombic phase may be the key ingredient to stabilize the stripe AF order.

Motivated by possible coupling between AF order and structural distortion, we examined if the strong magnetic field affects the formation of twinned orthorhombic domains. Since the AF moment, which is parallel to the orthorhombic *a*-direction, tends to align perpendicular to the external field, we expect that single domain structure may be achieved by field cooling. However, this was not successful. We have cooled the crystal in the magnetic field of 11 T applied along [110] direction of the tetragonal unit cell from 140 K down to 40 K. The angular variation of the NMR spectra at 40 K still showed two sets of satellite lines from twinned domains with roughly equal intensity.

We next discuss the anisotropic fluctuations observed in the relaxation rate measurements. Generally, $(T_1T)^{-1}$ can be expressed by the wave-vector-dependent dynamic spin susceptibility $\text{Im}\chi^\perp(q, \omega)$ and the hyperfine form factor $A_\perp(q)$ as

$$\frac{1}{T_1T} \propto \lim_{\omega \rightarrow 0} \sum_q A_\perp^2(q) \frac{\text{Im}\chi^\perp(q, \omega)}{\omega}. \quad (5)$$

Note that the relaxation rate, which is the transition probability between the nuclear spin levels, is determined by the component of the dynamic susceptibility perpendicular to the effective field. In the paramagnetic phase, enhancement of $(T_1T)^{-1}$ with decreasing temperature is observed only for $H \perp c$. Therefore, this must be due to the fluctuations of the hyperfine field along the *c*-direction. As discussed in the appendix, such fluctuations can be generated only from the stripe-type spin fluctuations along the *a*-direction. In other words, the fluctuations must be strongly anisotropic in the spin space. Since the fluctuations are observed in the tetragonal paramagnetic phase, they might play an important role in the superconductivity of the K-doped BaFe₂As₂, which does not exhibit transition to the orthorhombic or antiferromagnetic phases. If the stripe-type fluctuations exist in the superconducting materials, we expect the anisotropic enhancement of $(T_1T)^{-1}$ be observed in the ⁷⁵As-NMR experiment.

5. Conclusions

We have investigated the simultaneous magnetic and structural phase transition and magnetic fluctuations in the paramagnetic tetragonal phase in BaFe₂As₂ by ⁷⁵As-NMR, using a high quality single crystal grown by the

self-flux method. The spin structure in the AF ordered phase is determined almost uniquely to be of stripe type from the NMR spectra, in agreement with the neutron experiments.

The substantial symmetry change of the electric field gradient (EFG) tensor at the As nuclei at the transition indicates drastic change of the charge distribution associated with the hybridization of Fe-3d and As-4p orbitals in spite of the apparently small orthorhombic crystal distortion. The anisotropic nature of the Fe-As bonds may help to stabilize the stripe AF order. The EFG shows strong temperature dependence even within the tetragonal phase, indicating continuous change of the local charge distribution.

The NMR relaxation rates shows distinct behavior for different field orientations. The enhancement of $(T_1T)^{-1}$ for $H \perp c$ with decreasing temperature implies development of stripe antiferromagnetic fluctuations, which is anisotropic in spin space. Since the stripe AF order appears by a first-order transition, persistence of such fluctuations in the paramagnetic phase is unexpected. Since the paramagnetic phase of BaFe_2As_2 evolves continuously to the superconducting phase by K doping, the stripe fluctuations may play an important role for superconductivity. Whether this is the case or not should be examined by the anisotropy of the ^{75}As -NMR relaxation rates in the superconducting materials in future studies.

Acknowledgments

We thank R. Arita and Y. Matsushita for enlightening discussions, and Y. Kiuchi for the EDX analysis. This work was supported partly by Grant-in-Aids on Priority Areas ‘‘Invention of Anomalous Quantum Materials’’ (No. 16076204) and by Special Coordination Funds for Promoting Science and Technology Promotion of Environmental Improvement for Independence of Young Researchers from MEXT of Japan. K. K. and N. K. are financially supported as JSPS research fellows.

Appendix: Symmetry Analysis of the Hyperfine Coupling Tensor and the Spin Structure in the AF phase

We discuss the spin structure in the AF phase based on the general symmetry properties of the hyperfine coupling tensor. Since the long range dipolar interaction gives only small contribution to the internal field, we focus on the short range transferred hyperfine interaction between the As nucleus and ordered moments on the four nearest neighbor Fe sites (see Fig. A-1).

The internal field can be written as the sum of contributions from each Fe sites.

$$\mathbf{H}_{\text{int}} = \sum_{i=1}^4 \mathbf{B}_i \cdot \mathbf{m}_i, \quad (\text{A}\cdot 1)$$

where \mathbf{m}_i is the ordered moment at the i -th Fe site and \mathbf{B}_i is the hyperfine coupling tensor between the As nucleus and i -th Fe site. We explicitly write components of

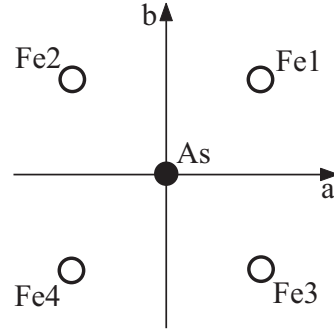


Fig. A-1. Coordination of the nearest neighbor Fe sites around an As nucleus in the orthorhombic unit cell. Note that As and Fe sites are not on the same plane.

\mathbf{B}_1 as

$$\mathbf{B}_1 = \begin{pmatrix} B_{aa} & B_{ab} & B_{ac} \\ B_{ba} & B_{bb} & B_{bc} \\ B_{ca} & B_{cb} & B_{cc} \end{pmatrix}. \quad (\text{A}\cdot 2)$$

Any component can be nonzero in the orthorhombic $Fmmm$ structure. The coupling tensor for other sites can be determined by symmetry consideration. For example, since the Fe2 site is related to the Fe1 site by mirror reflection with respect to the bc -plane, \mathbf{B}_2 is given as

$$\mathbf{B}_2 = \begin{pmatrix} B_{aa} & -B_{ab} & -B_{ac} \\ -B_{ba} & B_{bb} & B_{bc} \\ -B_{ca} & B_{cb} & B_{cc} \end{pmatrix}. \quad (\text{A}\cdot 3)$$

Likewise

$$\mathbf{B}_3 = \begin{pmatrix} B_{aa} & -B_{ab} & B_{ac} \\ -B_{ba} & B_{bb} & -B_{bc} \\ B_{ca} & -B_{cb} & B_{cc} \end{pmatrix},$$

$$\mathbf{B}_4 = \begin{pmatrix} B_{aa} & B_{ab} & -B_{ac} \\ B_{ba} & B_{bb} & -B_{bc} \\ -B_{ca} & -B_{cb} & B_{cc} \end{pmatrix}. \quad (\text{A}\cdot 4)$$

In the paramagnetic phase, the moment is uniform $\mathbf{m}_i = \mathbf{m}$, therefore, $\mathbf{H}_{\text{int}} = \left(\sum_{i=1}^4 \mathbf{B}_i \right) \cdot \mathbf{m}$, where

$$\sum_{i=1}^4 \mathbf{B}_i = 4 \begin{pmatrix} B_{aa} & 0 & 0 \\ 0 & B_{bb} & 0 \\ 0 & 0 & B_{cc} \end{pmatrix}. \quad (\text{A}\cdot 5)$$

The diagonal components in the paramagnetic state can be determined from the experimental K vs. χ plot as $B_{aa} = B_{bb} = 0.66 \text{ T}/\mu_B$, $B_{cc} = 0.47 \text{ T}/\mu_B$.

Let us now examine the internal fields for all possible antiferromagnetic structure.

(Case I): We first consider the stripe-order specified by the wave vector (100) or (101) shown in Fig. 6(a). In this case,

$$\mathbf{m}_1 = -\mathbf{m}_2 = \mathbf{m}_3 = -\mathbf{m}_4 \equiv \boldsymbol{\sigma}^I, \quad (\text{A}\cdot 6)$$

therefore,

$$\mathbf{H}_{\text{int}} = (\mathbf{B}_1 - \mathbf{B}_2 + \mathbf{B}_3 - \mathbf{B}_4) \cdot \boldsymbol{\sigma}^I. \quad (\text{A}\cdot 7)$$

Since

$$\mathbf{B}_1 - \mathbf{B}_2 + \mathbf{B}_3 - \mathbf{B}_4 = \begin{pmatrix} 0 & 0 & 4B_{ac} \\ 0 & 0 & 0 \\ 4B_{ca} & 0 & 0 \end{pmatrix}, \quad (\text{A}\cdot 8)$$

we obtain

$$\mathbf{H}_{\text{int}} = 4B_{ac} \begin{pmatrix} \sigma_c^{\text{I}} \\ 0 \\ \sigma_a^{\text{I}} \end{pmatrix}. \quad (\text{A}\cdot 9)$$

The internal field changes sign for the As site neighboring along the a -direction, resulting in the splitting of the NMR lines. In order to explain our NMR observation of the internal field parallel to the c -axis, the AF moment must be directed along the a -axis, which is perpendicular to the stripe direction. This is entirely consistent with the results of neutron diffraction experiments.¹⁰ If we take the magnitude of the AF moment determined from the neutron experiments, $\sigma_a^{\text{I}} = 0.87\mu_B$ the experimental result $\Delta = 1.5$ T leads to the value $B_{ac} = 0.43$ T/ μ_B .

(*Case II*): We next consider the Neel order specified by the wave vector (110) or (111), where $\mathbf{m}_1 = -\mathbf{m}_2 = -\mathbf{m}_3 = \mathbf{m}_4 \equiv \boldsymbol{\sigma}^{\text{II}}$. . Following the similar procedure, we have

$$\mathbf{H}_{\text{int}} = (\mathbf{B}_1 - \mathbf{B}_2 - \mathbf{B}_3 + \mathbf{B}_4) \cdot \boldsymbol{\sigma}^{\text{II}} \quad (\text{A}\cdot 10)$$

with

$$\mathbf{B}_1 - \mathbf{B}_2 - \mathbf{B}_3 + \mathbf{B}_4 = \begin{pmatrix} 0 & 4B_{ac} & 0 \\ 4B_{ac} & 0 & 0 \\ 0 & 0 & 0 \end{pmatrix}. \quad (\text{A}\cdot 11)$$

We then obtain

$$\mathbf{H}_{\text{int}} = 4B_{ab} \begin{pmatrix} \sigma_b^{\text{II}} \\ \sigma_a^{\text{II}} \\ 0 \end{pmatrix}. \quad (\text{A}\cdot 12)$$

Since the c -component of the internal field is zero for this case, it is not compatible with the NMR results.

(*Case III*): For completeness, we consider the ferromagnetic moment in the ab -plane specified by the wave vector (001) as displayed in Fig. 6(b). As far as the single layer is concerned, this case is identical to the paramagnetic state already considered. The internal field is then given

be

$$\Delta = 4B_{cc}\sigma_c^{\text{III}}, \quad (\text{A}\cdot 13)$$

where σ_c^{III} is the c -component of the AF moment for this case. The observed value $\Delta = 1.5$ T would then imply $\sigma_c^{\text{III}} = 0.80\mu_B$.

- 1) Y. Kamihara, T. Watanabe, M. Hirano, and H. Hosono: J. Am. Chem. Soc. **130** (2008) 3296.
- 2) C. de la Cruz, Q. Huang, J. Lynn, J. Li, W. R. II, J. Zarestky, H. Mook, G. Chen, J. Luo, N. Wang, and P. Dai: Nature **453** (2008) 899.
- 3) Y. Nakai, K. Ishida, Y. Kamihara, M. Hirano, and H. Hosono: J. Phys. Soc. Jpn. **77** (2008) 073701.
- 4) H. Kito, H. Eisaki, and A. Iyo: J. Phys. Soc. Jpn. **77** (2008) 063707.
- 5) J. Yang, Z. Li, W. Lu, W. Yi, X. Shen, Z. Ren, G. Che, X. Dong, L. Sun, F. Zhou, and Z. Zhao: Supercond. Sci. Technol. **21** (2008) 082001.
- 6) M. Rotter, M. Tegel, D. Johrendt, I. Schellenberg, W. Hermes, and R. Pöttgen: Phys. Rev. B **78** (2008) 020503(R).
- 7) M. Rotter, M. Tegel, and D. Johrendt: Phys. Rev. Lett. **101** (2008) 107006.
- 8) K. Sasmal, B. Lv, B. Lorenz, A. Guloy, F. Chen, Y. Xue, and C. W. Chu: cond-mat/0806.1301.
- 9) G. Wu, H. Chen, T. Wu, Y. Xie, Y. Yan, R. Liu, X. Wang, J. Ying, and X. Chen: cond-mat/0806.4279.
- 10) Q. Huang, Y. Qiu, W. Bao, J. Lynn, M. Green, Y. Gasparovic, T. Wu, G. Wu, and X. H. Chen: cond-mat/0806.2776.
- 11) X. F. Wang, T. Wu, G. Wu, H. Chen, Y. L. Xie, J. J. Ying, Y. J. Yan, R. H. Liu, and X. H. Chen: cond-mat/0806.2452.
- 12) A. Narath: Phys. Rev. **162** (1967) 320.
- 13) N. Ni, S. Bud'ko, A. Kreyssig, S. Nandi, G. E. Rustan, A. I. Goldman, S. Gupta, J. D. Corbett, A. Kracher, and P. Canfield: Phys. Rev. B **78** (2008) 014507.
- 14) G. C. Carter, L. H. Bennett, and D. J. Kahan: *Metallic Shifts in NMR* (Pergamon Press, Oxford, 1977)
- 15) S.-H. Baek, T. Klimczuk, F. Ronning, E. D. Bauer, N. Curro, and J. Thompson: cond-mat/0807.1084.
- 16) H. Fukazawa, K. Hirayama, K. Kondo, T. Yamazaki, Y. Kohori, N. Takeshita, K. Miyazawa, H. Kito, H. Eisaki, and A. Iyo: cond-mat/0806.4514.
- 17) K. Kaneko, A. Hoser, N. Caroca-Canales, A. Jesche, C. Krellner, O. Stockert, and C. Geibel: cond-mat/0807.2608.
- 18) A. Goldman, D. Argyriou, B. Ouladdiaf, T. Chatterji, A. Kreyssig, S. Nandi, N. Ni, S. Budko, P. Canfield, and R. McQueeney: cond-mat/0807.1525.